**EPJ manuscript No.**
(will be inserted by the editor)

# CLAS12 and its Science Program at the Jefferson Lab Upgrade.

## Selected Topics

Volker D. Burkert

Jefferson Lab, Newport News, Virginia, USA

November 7, 2008

**Abstract.** An overview of the CLAS12 detector is presented and the initial physics program after the energy-doubling of the Jefferson Lab electron accelerator. Construction of the 12 GeV upgrade project has started October 2008. A broad program has been developed to map the nucleon's 3-dimensional spin and flavor content through the measurement of deeply exclusive and semi-inclusive processes. Other programs include forward distribution function to large $x_B \leq 0.85$ and of the quark and gluon polarized distribution functions, and nucleon ground state and transition form factors at high $Q^2$. The 12 GeV electron beam and the large acceptance of CLAS12 are also well suited to explore hadronization properties using the nucleus as a laboratory.

**PACS.** 1 1.55.Fv, 13.60.Le, 13.40.Gp, 14.20.Gk



## 1 Introduction

The challenge of understanding nucleon electromagnetic structure still continues after more than five decades of experimental scrutiny. From the initial measurements of elastic form factors to the accurate determination of parton distributions through deep inelastic scattering (DIS), the experiments have increased in statistical and systematic accuracy. It was realized in recent years that the parton distribution functions represent special cases of a more general, and much more powerful way of characterizing the structure of the nucleon, the generalized parton distributions (GPDs) [1,2,3,4].

The GPDs describe the simultaneous distribution of particles with respect to both position and momentum. In addition to the information about the spatial density (form factors) and momentum density (parton distribution), these functions reveal the correlation of the spatial and momentum distributions, *i.e.* how the spatial shape of the nucleon changes when probing quarks of different wavelengths.

The concept of GPDs has led to completely new methods of "spatial imaging" of the nucleon, either in the form of two-dimensional tomographic images, or in the form of genuine three-dimensional images. GPDs also allow us to quantify how the orbital motion of quarks in the nucleon contributes to the nucleon spin – a question of crucial importance for our understanding of the "mechanics" underlying nucleon structure. The spatial view of the nucleon enabled by the GPDs provides us with new ways to test dynamical models of nucleon structure.

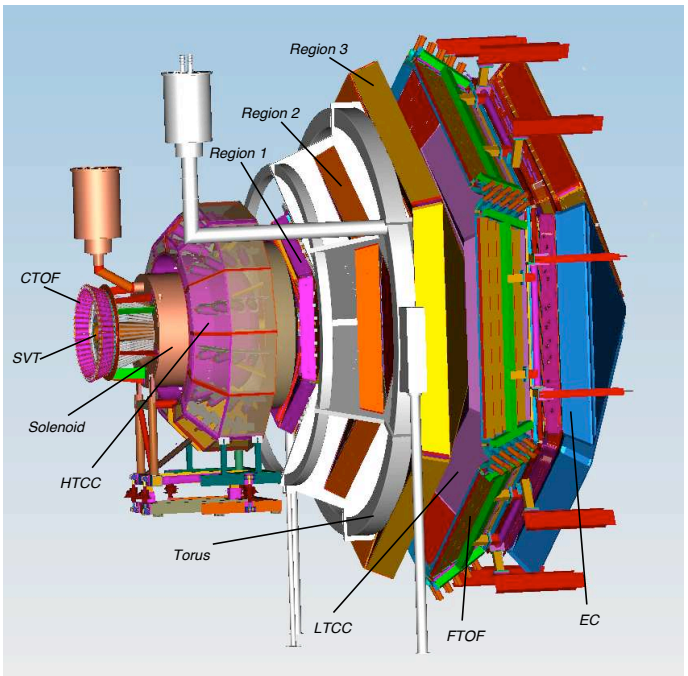


**Fig. 1.** 3D view of the CLAS12 detector. The beam comes from the left. The target is located inside the superconducting solenoid magnet.

The mapping of the nucleon GPDs, and a detailed understanding of the spatial quark and gluon structure of the nucleon, have been widely recognized as the key objectives of nuclear physics of the next decade. This requires a com-

prehensive program, combining results of measurements of a variety of processes in electron–nucleon scattering with structural information obtained from theoretical studies, as well as with expected results from future lattice QCD simulations.

While GPDs, and also the recently introduced transverse momentum dependent distribution functions (TMDs), open up new avenues of research, the traditional means of studying the nucleon structure through electromagnetic elastic and transition form factors, and through flavor- and spin-dependent parton distributions must also be employed with high precision to extract physics on the nucleon structure in the transition from the regime of quark confinement to the domain of asymptotic freedom. These avenues of research can be explored using the 12 GeV cw beam of the JLab upgrade with much higher precision than has been achieved before, and can help reveal some of the remaining secrets of QCD. Also, the high luminosity available will allow us to explore the regime of extreme quark momentum, where a single quark carries 80% or more of the proton's total momentum.

## 2 The CLAS12 Detector

To meet the requirements of high statistics measurements for exclusive processes the equipment at JLab will undergo major upgrades. In particular it will include the CLAS12 large acceptance spectrometer [54], which is shown in Fig. 1. The main new features of CLAS12 include operation with a luminosity of $10^{35}$cm$^{-2}$sec$^{-1}$, an order of magnitude increase over previous CLAS [5], and improved particle identification capabilities at more forward angles. CLAS12 has two major parts with different functions, the Forward Detector (FD) and the Central Detector (CD). I this section I present a short descriptions of the detector system.

### 2.1 The Forward Detector

Improved electron-pion separation at higher momentum is achieved with a gas Cherenkov counter with a pion momentum threshold of 4.9 GeV/c. The new high threshold Cherenkov counter (HTCC) is positioned in front of a superconducting toroidal magnet, and has to present as little material to the charged particles as practical to limit multiple scattering contributing to the momentum resolution. This requires use of low mass composite material for the mirror system.

The HTCC is followed by a toroidal magnet for the momentum analysis of tracks with scattering angles from 5° to 40°. Similar to CLAS the new toroidal magnet has six superconducting symmetrically arranged around the beam line, and provides six sectors for charged particle detection. In each sectors tracking is accomplished with a set of 3 regions of drift chambers with 12 layers of hexagoal drift cells arranged at stereo angles of ±6°. This arrangement provides good angular resolution both in polar angle and in azimuthal angle. The drift chamber system will provide 36 measurements for a single charged track and has sufficient redundancy for pattern recognition and track reconstruction.

The Torus magnet and the drift chamber system are followed by the low-threshold Cherenkov counter (LTCC) that provides charged pion identification for momenta greater than 3 GeV/c. Following the LTCC are two arrays of plastic scintillators for charged particle identification. The first layer contains 22 strips of 5cm thick and 15 cm wide scintillator strips and provides timing information of 150psec. The second layer is 6 cm thick and has 6 cm wide strips. It provides improved timing information of $\delta T < 100$ psec due to the better light collection. A combined resolution of 80 psec is expected. For equal pion, kaon, and proton yields this will enable a $4\sigma$ $\pi$/K separation up to 3 GeV/c, and a K/p separation up to 4.5 GeV/c from time-of-flight measurements. A future upgrade of the particle identification is under consideration that would replace one or more of the LTCC sectors with RICH detectors that will allow much improved identification of pions, kaons and protons at high momentum where time-of-flight measurements are less effective.

Large parts of the physics program require the identification of single high energy photons and separation from $\pi^\circ \rightarrow \gamma\gamma$ up to 9 GeV/c. The granularity of the existing electromagnetic calorimeter (EC) will be improved by adding a preshower calorimeter of 5-6 radiation length (PCAL) in front of EC that provides a factor 2.5 better spatial resolution and a separation of two photons up to momenta greater 10 GeV/c. At forward angles below 6°, a lead-tungstate calorimeter consisting of 420 crystals with an average cross section of 15mm x 15mm and 18 rad. length thick, provides photon and $\pi^\circ$ identification for momenta up to 10 GeV/c.

### 2.2 The Central Detector

The Central Detectors (CD) is based on a compact solenoid magnet with maximum central magnetic field of 5 Tesla. The solenoid magnets provides momentum analysis for polar angles greater than 35°, protection of tracking detectors from background electrons, and acts as a polarizing field for dynamically polarized solid state targets. All three functions require high magnetic field. The overall size of the solenoid is restricted to 200 cm in diameter which allows a maximum warm bore for the placement of detectors of 80 cm. To obtain sufficient momentum resolution in the limited space available requires high field and excellent position resolution of the tracking detectors. The central field in the target region must also be very uniform at $\Delta B/B < 10^{-4}$ to allow the operation of a dynamically polarized target. To achieve a sustained high polarization for polarized ammonia targets requires magnetic fields in excess of 3 T. Magnetic Fields of 5 T have been most recently used for such targets with polarization of 80% - 90% for hydrogen. In addition, the solenoidal field provides the ideal guiding field for keeping the copiously produced Möller electrons away from the sensitive detectors

and guide them to downstream locations where they can be passively absorbed in high-Z material.

Tracking in the CD is provided by a silicon vertex tracker (SVT) that uses silicon strip technology and provides tracking for polar angle from 5° to 135°. The tracker consists of a barrel strip tracker (BST) and a forward detecor (FST). The BST has 8 stereo layers of silicon sensors and provides standalone tracking for polar angle from $35^circ$ to 135°. The FST has 6 stereo layers and covers the range from 5° to 35° and acts together with the forward drift chamber tracking system to significantly improve vertex resolution and momentum resolution.

The central time-of-flight scintillator array (CTOF) consists of 50 strips of fast plastic scintillator equipped with 100 photomultipliers that provide 2-sided light readout. The scintillator light is brought to an area of reduced magnetic field where either PMTs with lower magnetic field sensitivity can be used or where passive shielding can be employed. R&D work is still underway to study these options.

The very short flight path available allows for particle identification in a restricted momentum range of up to 1.2 GeV/c and 0.65 GeV/c for pion-proton and pion-kaon separation, respectively.

Several possible upgrades of the CD are currently being studied: a significant improvement in tracking resolution is possible by adding several layers of micromegas detectors to the barrel part of the SVT, and replacing two of the SVT layers by micromegas. This option is currently under study at CEA Saclay. Also under study by a French-Italian collaboration is an additional detector that will add neutral particle detection capabilities, for example for the study of DVCS on neutrons, using a liquid deuterium target. This detector will fill the gap between the CTOF and the solenoid cryostat.

With these upgrades `CLAS12` will be the work horse for exclusive and semi-inclusive electroproduction experiments in the deep inelastic kinematics.

In the following sections I describe the currently anticipated initial physics program for CLAS12.

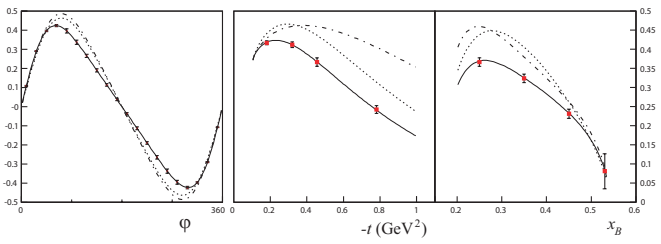


**Fig. 2.** The beam spin asymmetry showing the DVCS-BH interference for 11 GeV beam energy [7]. Left panel: $x = 0.2$, $Q^2 = 3.3\text{GeV}^2$, $-t = 0.45\text{GeV}^2$. Middle and right panels: $\phi = 90°$, other parameters same as in left panel. Many other bins will be measured simultaneously. The curves represent various parameterizations within the VGG model [6]. Projected uncertainties are statistical.

## 3 Generalized Parton Distributions and DVCS

It is now well recognized [1,8,9,10] that deeply virtual Compton scattering and deeply virtual meson production are most suitable for mapping out the twist-2 vector GPDs $H,\ E$ and the axial GPDs $\tilde{H},\ \tilde{E}$ in $x,\ \xi,\ t$, where $x$ is the momentum fraction of the struck quark, $\xi$ the longitudinal momentum transfer to the quark, and $t$ the transverse momentum transfer to the nucleon. Having access to a 3-dimensional image of the nucleon (two dimensions in transverse space, one dimension in longitudinal momentum) opens up completely new insights into the complex structure of the nucleon. In addition, GPDs carry information of more global nature. For example, the nucleon matrix element of the energy-momentum tensor contains 3 form factors that encode information on the angular momentum distribution $J^q(t)$ of the quarks with flavor $q$ in transverse space, their mass-energy distribution $M_2^q(t)$, and their pressure and force distribution $d_1^q(t)$. How can we access these form factors? The only known process to directly measure them is elastic graviton scattering off the nucleon. However, these form factors also appear as moments of the vector GPDs [11], thus offering prospects of accessing gravitational form factors through the detailed mapping of GPDs. The quark angular momentum in the nucleon is given by

$$J^q(t) = \int_{-1}^{+1} dx x[H^q(x,\xi,t) + E^q(x,\xi,t)] \ ,$$

and the mass-energy and pressure distribution

$$M_2^q(t) + 4/5 d_1^q(t)\xi^2 = \int_{-1}^{+1} dx x H^q(x,\xi,t) \ .$$

The mass-energy and force-pressure distribution of the quarks are given by the second moment of GPD $H$, and their relative contribution is controlled by $\xi$. A separation of $M_2^q(t)$ and $d_1^q(t)$ requires measurement of these moments in a large range of $\xi$. The beam helicity-dependent cross section asymmetry is given in leading twist as

$$A_{LU} \approx \sin\phi[F_1(t)H + \xi(F_1+F_2)\tilde{H}]d\phi \ ,$$

where $\phi$ is the azimuthal angle between the electron scattering plane and the hadronic plane. The kinematically suppressed term with GPD $E$ is omitted. The asymmetry is mostly sensitive to the GPD $H(x=\xi,\xi,t)$. In a wide kinematics [12,13] the beam asymmetry $A_{LU}$ was measured at Jefferson Lab at modestly high $Q^2$, $\xi$, and $t$, and in a more limited kinematics [14] the cross section difference $\Delta\sigma_{LU}$ was measured with high statistics. Moreover, a first measurement of the target asymmetry $A_{UL} = \Delta\sigma_{UL}/2\sigma$ was carried out [15], where

$$A_{UL} \approx \sin\phi[F_1\tilde{H} + \xi(F_1+F_2)H] \ .$$

The combination of $A_{LU}$ and $A_{UL}$ allows to separate GPD $H(x=\xi,\xi,t)$ and $\tilde{H}(x=\xi,\xi,t)$. Using a transversely polarized target the asymmetry

$$A_{UT} \approx \cos\phi\sin(\phi-\phi_s)[t/4M^2(F_2H - F_1E)]$$

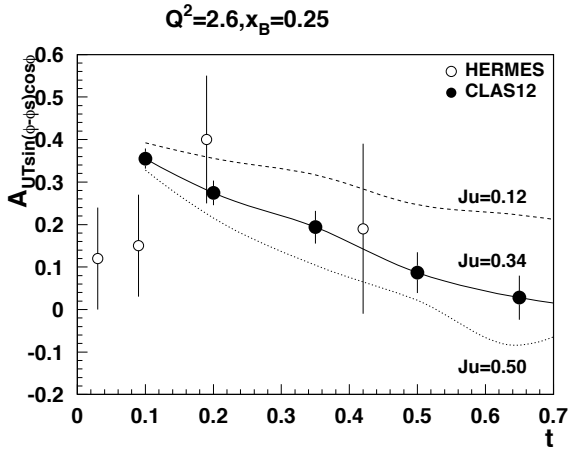


**Fig. 3.** Projected transverse target asymmetry $A_{UT}$ for DVCS production off protons at 11 GeV beam energy.

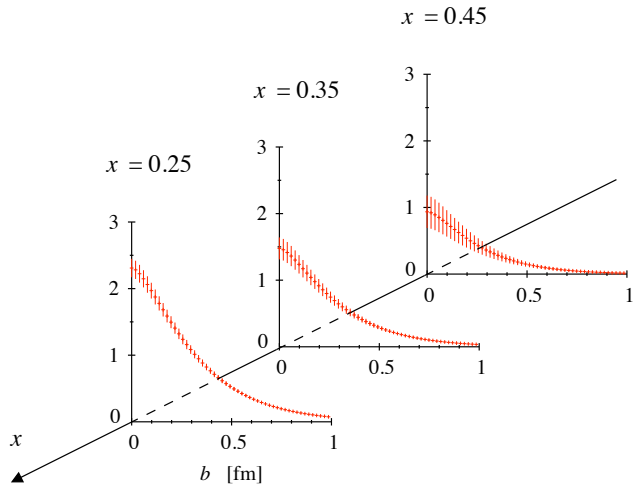


**Fig. 4.** The u-quark distribution in transverse space as extracted from projected DVCS data with CLAS12.

can be measured, where $\phi_s$ is the azimuthal angle of the target polarization vector relative to the electron scattering plane. $A_{UT}$ depends in leading order on GPD $E$.

First DVCS experiments carried out at JLab [12,15, 14,13] and DESY [16] showed promising results in terms of the applicability of the handbag mechanism to probe GPDs. The 12 GeV upgrade offers much improved possibilities for accessing GPDs. Figure 2 shows the expected statistical precision of the beam DVCS asymmetry for some sample kinematics. Using a polarized target one can also measure the target spin asymmetries with high precision. Figure 3 shows the expected statistical accuracy for one kinematics bin. A measurement of all 3 asymmetries will allow a separate determination of GPDs $H$, $\tilde{H}$ and $E$ at the above specified kinematics. Through a Fourier transformation the t-dependence of GPD $H$ can be used to determine the $u-$quark distribution in transverse impact parameter space. Figure 4 shows projected results.

Deeply virtual meson production will play an important role in disentangling the flavor- and spin-dependence of GPDs. For exclusive mesons only the longitudinal photon coupling in $\gamma^* p \to Nm$ enables direct access to GPDs through the handbag mechanism and must be isolated from the transverse coupling. That the transverse contribution cannot be neglected at currently available energies of 6 GeV was observed in the non-zero beam asymmetry measured with CLAS [17] that indicated the presence of a significant longitudinal-transverse interference term in the amplitudes. In addition, the dominance of the handbag mechanism in the longitudinal cross section must first be established at the upgrade energy.

## 4 Transverse momentum dependent parton distributions and SIDIS

Semi-inclusive deep inelastic scattering (SIDIS) studies, when a hadron is detected in coincidence with the scattered lepton that allows "flavor tagging", provide more direct access to contributions from different quark species. In addition, they give access to the transverse momentum distributions of quarks, not accessible in inclusive scattering. Azimuthal distributions of final state particles in semi-inclusive deep inelastic scattering provide access to the orbital motion of quarks and play an important role in the study of TMDs of quarks in the nucleon.

| N/q | U | L | T |
|---|---|---|---|
| U | $\mathbf{f_1}$ | | $h_1^\perp$ |
| L | | $\mathbf{g_1}$ | $h_{1L}^\perp$ |
| T | $f_{1T}^\perp$ | $g_{1T}$ | $\mathbf{h_1}$ $h_{1T}^\perp$ |

**Table 1.** Leading-twist transverse momentum-dependent distribution functions. $U$, $L$, and $T$ stand for transitions of unpolarized, longitudinally polarized, and transversely polarized nucleons (rows) to corresponding quarks (columns).

TMD distributions (see Table 1) describe transitions of a nucleon with one polarization in the initial state to a quark with another polarization in the final state. The diagonal elements of the table are the momentum, longitudinal and transverse spin distributions of partons, and represent well-known parton distribution functions related to the square of the leading-twist, light-cone wave functions. Off-diagonal elements require non-zero orbital angular momentum and are related to the wave function overlap of $L$=0 and $L$=1 Fock states of the nucleon [18]. The chiral-even distributions $f_{1T}^\perp$ and $g_{1T}$ are the imaginary parts of the corresponding interference terms, and the chiral-odd $h_1^\perp$ and $h_{1L}$ are the real parts. The TMDs $f_{1T}^\perp$ and $h_1^\perp$, which are related to the imaginary part of the interference of wave functions for different orbital momentum states and are known as the Sivers and Boer-Mulders functions, and describe unpolarized quarks in the

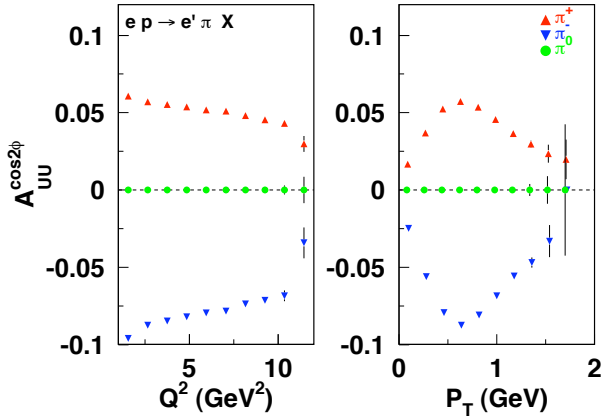


**Fig. 5.** The $\cos 2\phi$ moment (Boer-Mulders asymmetry) for pions as a function of $Q^2$ and $P_T$ for $Q^2 > 2$ GeV$^2$ (right) with CLAS12 at 11 GeV from 2000 hours of running. Values are calculated assuming $H_1^{\perp u\to\pi^+} = -H_1^{\perp u\to\pi^-}$. Only statistical uncertainties are shown.

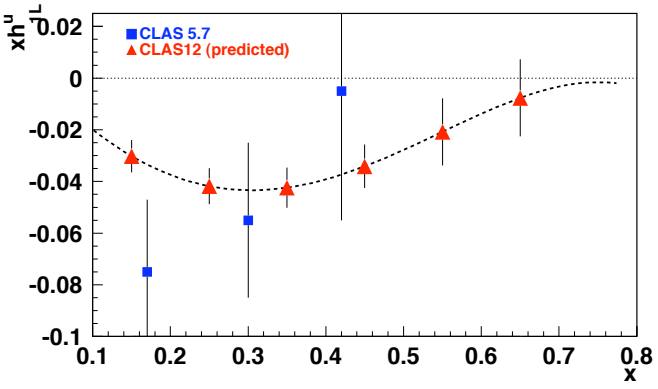


**Fig. 6.** Projected data from CLAS12 for the chiral odd function $h_{1L}^u$ for $u$-quarks.

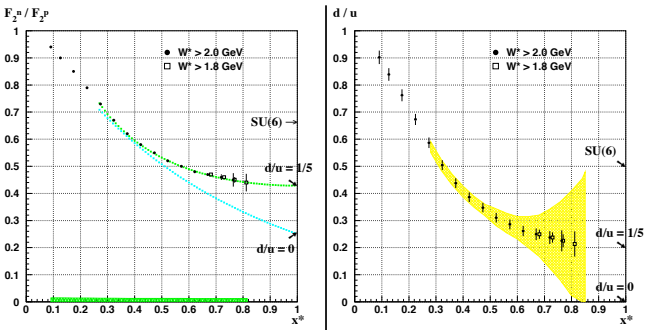


**Fig. 7.** Projected data for the ratio $F_2^n/F_2^p$ (left) and $d/u$ (right) for 11 GeV beam energy [22]. The error bars in the right panel contain both statistical and systematic uncertainties. The yellow area shows the uncertainty of current data due to poorly known nuclear corrections.

transversely polarized nucleon and transversely polarized quarks in the unpolarized nucleon respectively. The most simple mechanism that can lead to a Boer-Mulders function is a correlation between the spin of the quarks and their orbital angular momentum. In combination with a final state interaction that is on average attractive, already a measurement of the sign of the Boer-Mulders function, would thus reveal the correlation between orbital angular momentum and spin of the quarks.

Similar to GPDs, TMD studies will benefit from the higher energy and high luminosity at 12 GeV. A comprehensive program is in preparation with CLAS12 to study the new structure functions. Examples of expected uncertainties [20] for the Boer-Mulders asymmetry $A_{UU}^{cos2\phi}$ are presented in Fig. 5. Projections of the Mulders function $h_{1L}^u$ for $u-$quarks from $\pi^+$ asymmetries $A_{UL}$ with CLAS12 are shown in Fig. 6, and compared with preliminary results from the CLAS EG1 data set at 5.75 GeV beam energy.

## 5 Inclusive structure functions and moments

Polarized and unpolarized structure functions of the nucleon offer a unique window into the internal quark structure of baryons. The study of these structure functions provides insight into the two defining features of QCD — asymptotic freedom at small distances, and confinement and non-perturbative effects at large distance scales. After more than three decades of measurements at many accelerator facilities worldwide, a truly impressive amount of data has been collected, covering several orders of magnitude in both kinematic variables $x$ and $Q^2$. However, there are still important regions of the accessible phase space where data are scarce and have large errors and where significant improvements are possible through precise experiments at Jefferson Lab.

One of the open questions is the behavior of the structure functions in the extreme kinematic limit $x \to 1$. In this region effects from the virtual sea of quark-antiquark pairs are suppressed, making this region simpler to model. This is also the region where pQCD can make absolute predictions. However, the large $x$ domain is hard to reach because cross sections are kinematically suppressed, the parton distributions are small and final states interactions (partonic or hadronic) are large. First steps into the large $x$ domain became possible at energies of 5-6 GeV [21,23, 24,25]. The interest triggered by these first results and the clear necessity to extend the program to larger $x$ provided one of the cornerstone of the JLab 12 GeV upgrade physics program.

### 5.1 Valence quark structure and flavor dependence at large $x$.

The unpolarized structure function $F_2^p(x)$ has been mapped out in a large range of $x$ leading to precise knowledge of

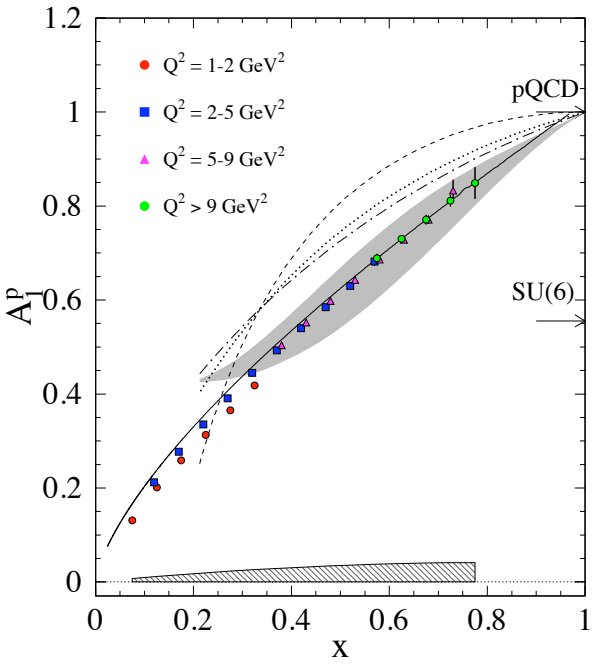


**Fig. 8.** Anticipated results on $A_1^p$.The four different symbols represent four different $Q^2$ ranges. The statistical uncertainty is given by the error bars while the systematic uncertainty is given by the shaded band.

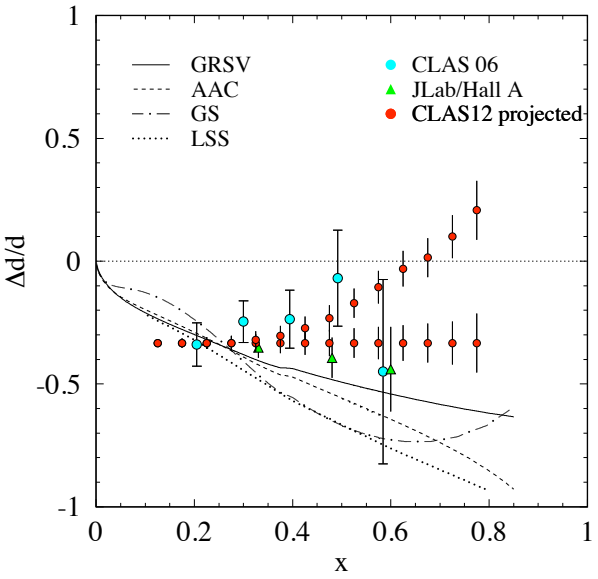


**Fig. 9.** Expected results for $(\Delta d + \Delta\bar{d})/(d + \bar{d})$. The central values of the data are following two arbitrary curves to demonstrate how the two categories of predictions, namely the ones that predict $\Delta d/d$ stays negative (LO and NLO analyses of polarized DIS data: GRSV, LSS, AAC, GS, statistical model, and a quark-hadron duality scenario) and the ones predicting $\Delta d/d \to 1$ when $x \to 1$ (leading order pQCD and a quark-hadron duality scenario).

the quark distribution $u(x)$. The corresponding structure function $F_2^n(x)$ is, however, well measured only for $x < 0.5$ as nuclear corrections, when using deuterium as a target, become large at large $x$ and are not well represented by Fermi motion. At JLab a new technique tested recently with `CLAS` has been shown to be very effective in reducing the nuclear corrections. The `BONUS` experiment [21] has recently taken data using a novel radial TPC with GEM readout as detector for the low-energy spectator proton in the reaction $en(p_s) \to ep_sX$. Measurement of the spectator proton for momenta as low as 70 MeV/c and at large angles minimizes the poorly known nuclear corrections at large $x$. The techniques can be used with `CLAS12` at 12 GeV to accurately determine the ratio $d(x)/u(x)$ to much larger $x$ values. Figure 7 shows the projected data for $F_2^n(x)/F_2^p(x)$ and $d(x)/u(x)$. A dramatic improvement can be achieved at large $x$.

### 5.2 Spin structure functions and parton distributions

The JLab PAC30 also approved E12-06-109 [26] which will specifically study polarized parton distributions at large $x$. Using standard detection equipment, a redesigned polarized target adapted to `CLAS12` and 30 (50) days of running on a longitudinally polarized $NH_3$ ($ND_3$) target, high precision measurements can be achieved as shown in Fig. 8. These data will disentangle models in the large-$x$ region. While the results shown in Fig. 8 are with a $W > 2$ GeV constraint, hadron-parton duality studies will tell us by how much this constraint can be relaxed, possibly increasing the $x$ range up to 0.9. The expected accuracy for $(\Delta d + \Delta\bar{d})/(d + \bar{d})$ is shown in Fig. 9.

### 5.3 Global Fit of Polarized Parton Distributions

The large window that wil open up over the DIS domain with the 12 GeV upgrade will permit constraints of global fits of the parton distributions. JLab data at lower energies had already unique impact at large $x$. The improvement from the 12-GeV upgrade is also significant at low and moderate $x$, noticeably for the polarized gluon distribution $\Delta G$. To demonstrate the precision achievable with the expected `CLAS12` data, we have plotted in Fig. 10 a study of the expected impact of expected JLab data on the NLO analyses of the polarized gluon distribution [27]. A dramatic improvement can be achieved with the expected data from the `CLAS12` proposal E12-06-109 [26]. We emphasize that the data will not only reduce the error band on $\Delta G$, but will likely allow a more detailed modeling of its $x$-dependence. Significant improvements are expected for the quark distributions as well.

### 5.4 Moments of spin structure functions.

Moments of structure functions provide powerful insight into nucleon structure. Inclusive data at JLab have permitted evaluation of the moments at low and intermediate $Q^2$ [28,29,30]. With a maximum beam energy of 6 GeV,

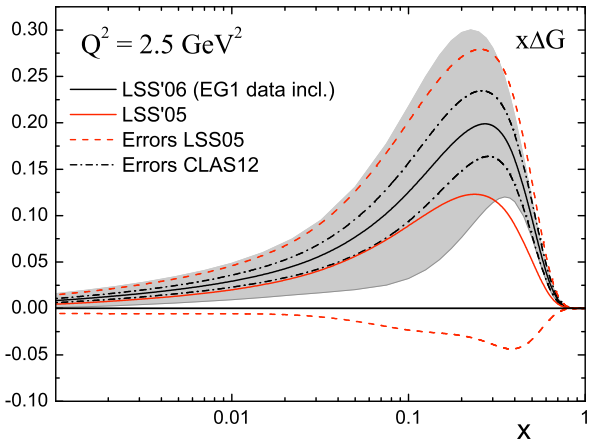


**Fig. 10.** Expected uncertainties for $x\Delta G$. The black solid curve shows the central value of the present analysis that includes CLAS EG1 data. The dashed-dotted lines give the error band when the expected `CLAS12` data are included in the LSS QCD analysis.

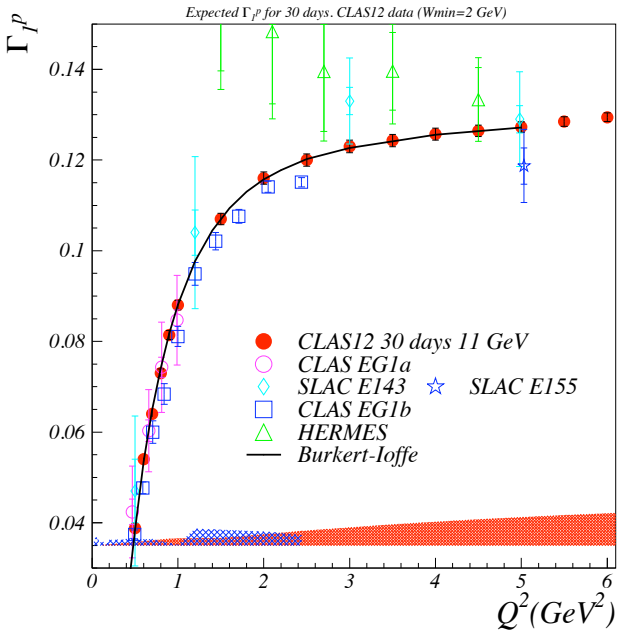


**Fig. 11.** Left plot: expected precision on $\Gamma_1^p$ for `CLAS12` and 30 days of running. `CLAS` EG1a [28,29] data and preliminary results from EG1b are shown for comparison. The data and systematic uncertainties include estimates of the unmeasured DIS contribution. HERMES [31] data, and E143 [32] and E155 data [33] from SLAC are also shown (including DIS contribution estimates). The model is from Burkert and Ioffe [35,36].

however, the measured strength of the moments becomes rather limited for $Q^2$ greater than a few GeV$^2$. The 12-GeV upgrade removes this problem and allows for measurements to higher $Q^2$.

Moments of structure functions are related to the nucleon static properties by sum rules. At large $Q^2$ the Bjorken sum rule relates the integral $\Gamma_1^{p-n} = \int (g_1^p - g_1^n) dx$ to the nucleon axial charge [34]. Figure 11 shows the expected precision on $\Gamma_1^p$. Published results and preliminary results from EG1b are also displayed for comparison. The hatched blue band corresponds to the systematic uncertainty on the EG1b data points. The red band indicates the estimated systematic uncertainty from `CLAS12`. The systematic uncertainties for EG1 and `CLAS12` include the estimated uncertainty on the unmeasured DIS part estimated using the model from Bianchi and Thomas [37]. As can be seen, moments can be measured up to $Q^2$=6 GeV$^2$ with a statistical accuracy improved several fold over that of the existing world data.

Finally, moments in the low ($\simeq 0.5$ GeV$^2$) to moderate ($\simeq$4 GeV$^2$) $Q^2$ range enable us to extract higher-twist parameters, which represent correlations between quarks in the nucleon. This extraction can be done by studying the $Q^2$ evolution of first moments [38,39]. Higher twists have been consistently found to have, overall, a surprisingly smaller effect than expected. Going to lower $Q^2$ enhances the higher-twist effects but makes it harder to disentangle a high twist from the yet higher ones. Furthermore, the uncertainty on $\alpha_s$ becomes prohibitive at low $Q^2$. Hence, higher twists turn out to be hard to measure, even at the present JLab energies. Adding higher $Q^2$ to the present JLab data set removes the issues of disentangling higher twists from each other and of the $\alpha_s$ uncertainty. The smallness of higher twists, however, requires statistically precise measurements with small point-to-point correlated systematic uncertainties. Such precision at moderate $Q^2$ has not been achieved by the experiments done at high energy accelerators, while JLab at 12 GeV presents the opportunity to reach it considering the expected statistical and systematic uncertainties of E12-06-109. The total point-to-point uncorrelated uncertainty on the twist-4 term for the Bjorken sum, $f_2^{p-n}$, decreases by a factor of 5-6 compared to results obtained in Ref. [40].

## 6 Nucleon form factors and resonance transitions at short distances

The most basic observables that reflect the composite nature of the nucleon are its electromagnetive form factors. Historically the first direct indication that the nucleon is not elementary comes from measurements of these quantities in elastic *ep* scattering [41]. The electric and magnetic form factors characterize the distributions of charge and magnetization in the nucleon as a function of spatial resolving power. The transition form factors reveal the nature of the excited states of the nucleon. Further, these quantities can be described and related to other observables through the GPDs.

Measurements of the elastic form factors will remain an important aspect of the physics program at 12 GeV, and will be part of the program in other experiments at JLab. The magnetic form factor of the neutron, as well as the

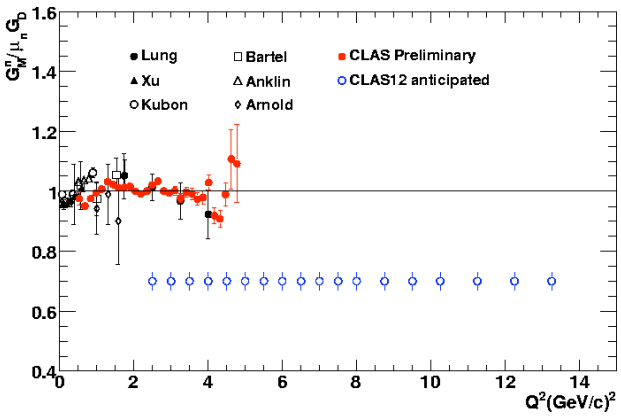


**Fig. 12.** The magnetic form factor for the neutron. The existing data, and projected uncertainties at 12 GeV with `CLAS12` (blue open circles).

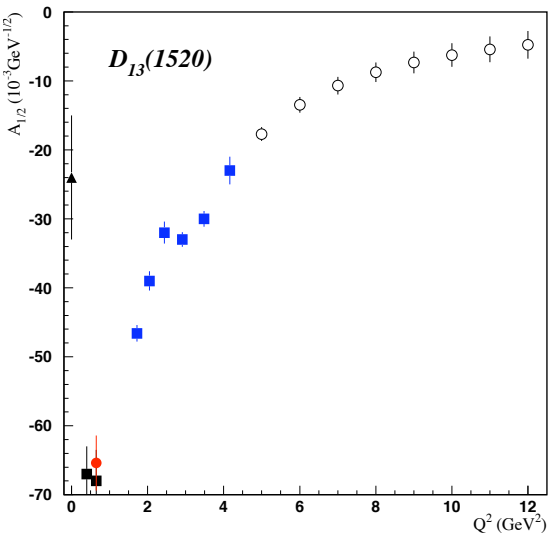


**Fig. 13.** The transverse photocoupling amplitude $A_{1/2}$ for the $N(1520)D_{13}$ resonance. The blue full squares are preliminary data from CLAS. The open circles represent projected results with `CLAS12` at 12 GeV.

transition form factors for several prominent resonances require special experimental setups for which `CLAS12` is suited best. Figure 12 shows the current data as well as the extension in $Q^2$ projected for the 12 GeV program with `CLAS12`.

Nucleon ground and excited states represent different eigenstates of the Hamiltonian, therefore to understand the interactions underlying nucleon formation from fundamental constituents, the structure of both the ground state and the excited states must be studied. The current $N^*$ program at Jlab has already generated results for the transition form factors at $Q^2$ up to 6 GeV$^2$ for the $\Delta(1232)$ [42, 43, 44], and up to 4 GeV$^2$ for the $N(1535)S_{11}$ [45, 46, 47]. The most recent results [48, 49] on the transition form factors for the Roper resonance $N(1440)P_{11}$ for $Q^2$ up to 4.5 GeV$^2$, have demonstrated the sensitivity to the degrees of freedom that are effective in the excitation of particular states. The JLab energy upgrade will allow us to probe resonance excitations at much higher $Q^2$, where the relevance of elementary quarks in the resonance formation may become evident through the approach to asymptotic scaling. Figure 13 shows projected $Q^2$ dependence of the $A_{1/2}$ transition amplitude for the $N(1520)D_{13}$ resonance obtained from single pion production. Higher mass resonances may be efficiently measured in double-pion processes [50, 51] such as $ep \rightarrow ep\pi^+\pi^-$.

## 7 Quarks and hadrons in the nuclear medium

### 7.1 Color Transparency

Color transparency (CT) is a unique prediction of QCD, and implies that under the right conditions, the nuclear medium will allow the transmission of hadrons with reduced absorption. The phenomenon of CT is predicted on the quark-gluon basis and is totally unexpected on a hadronic interaction picture. Three ingredients are necessary to observe CT: (1) the interactions must create a small size object (point-like configuration, PLC) that (2) has a small cross section when traveling in a hadronic medium, and (3) the distance over which it expands to its full hadronic size must be larger than the nucleus size. Such conditions require high enough energy transfer to the target where the photon couples to PLCs, and the full hadronization occurs outside the nucleus. The energy doubling of the electron accelerator to 12 GeV will provide conditions where a significantly increased transparency should be observable. Small increases in nuclear transparency consistent with theoretical predictions have been observed at JLab with 5-6 GeV electron beams in pion production [52], and in $\rho^\circ$ electroproduction with CLAS [53]. At 12 GeV much more significant changes of nuclear transparency are predicted and can be observed with high sensitivity in CLAS12 as shown in Fig. 14.

### 7.2 Hadronization

The use of electron beams at 12 GeV allows us to address fundamental questions of how colored quarks struck in the interaction with high energy photons transform into colorless hadrons. Questions that we want to have answered are, how long can a light colored quark remain deconfined? The production time $T_p$ measured this quantity. Since deconfined quarks emit gluons, $T_p$ can be measured via medium-stimulated gluon emission resulting in a broadening of the transverse momentum distribution of the final hadrons. Another important question to address is: How long does it take to form the color field of a hadron? This can be measured by the formation time $T_f^h$. Since hadrons interact strongly with the nuclear medium, $T_f^h$ can be determined by measuring the attenuation of hadrons in the nuclear medium by using nuclei of different sizes.

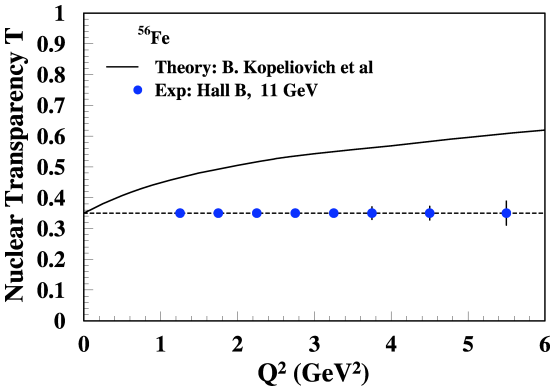


**Fig. 14.** Projected color transparency effects in Fe. The open circles represent projected results with CLAS12 at 12 GeV.

These question can be addressed by measuring the hadronic multiplicity ratio

$$R_M^h(z,\nu,p_T^2,Q^2,\phi) = \frac{\{\frac{N_h^{DIS}(z,\nu,p_T^2,Q^2,\phi)}{N_e^{DIS}(\nu,Q^2)}\}_A}{\{\frac{N_h^{DIS}(z,\nu,p_T^2,Q^2,\phi)}{N_e^{DIS}(\nu,Q^2)}\}_D}$$

versus all kinematical quantities.

## 8 Conclusions

The JLab energy upgrade and the planned new experimental equipment are well matched to an exciting scientific program aimed at studies of the complex nucleon structure in terms of the newly discovered longitudinal and transverse momentum dependent parton distribution functions, the GPDs and TMDs. They provide fundamentally new insights in the complex multi-dimensional structure of the nucleon. In addition, the high precision afforded by the high luminosity and the large acceptance detectors, and the development of novel techniques to measure scattering off nearly free neutrons, will enable the exploration of phase space domains with extreme conditions that could not be studied before. The CLAS12 detector will play a crucial role in exciting program.

### Acknowledgment

I am grateful to members of the CLAS collaboration who contributed to the development of the exciting physics program for the JLab upgrade to 12 GeV, and the CLAS12 detector. Much of the material in this report is taken from the CLAS12 Technical Design Report Version 3, October 2007 [54].

This work was supported in part by the U.S. Department of Energy and the National Science Foundation, the French Commisariat á l'Energie Atomique, the Italian Instituto Nazionale di Fisica Nucleare, the Korea Research Foundation, and a research grant of the Russian Federation. The Jefferson Science Associates, LLC, operates Jefferson Lab under contract DE-AC05-060R23177.

## References

1. X. Ji, Phys. Rev. D**55**, 7114, 1997.
2. X. Ji, Phys. Rev. Lett.**8**, 610, 1997.
3. A. Radyushkin, Phys. Lett. B**380**, 417, 1996.
4. A. Radyushkin, Phys. Rev. D**56**, 5524, 1997
5. B. Mecking et al., Nucl. Inst. Meth. A**503**,513, 2003.
6. M. Vanderhaeghen, P. Guichon, M. Guidal, Phys. Rev. D**60**, 094017, 1999.
7. JLAB experiment E12-06-119, F. Sabatie *et al.*
8. A. Belitsky, D. Mueller, A. Kirchner, Nucl. Phys. B**629**, 323, 2002.
9. M. Burkardt, Int. J. Mod. Phys. A**18**, 173, 2003.
10. A.V. Belitsky, X. Ji, F. Yuan, Phys. Rev. D**69**, 074014, 2004.
11. K. Goeke *et al.*, Phys. Rev. D**75**, 094021, 2007.
12. S. Stepanyan *et al.*, Phys. Rev. Lett.**87**, 182002, 2001.
13. F.X. Girod, *et al.*, Phys. Rev. Lett.**100**, 162002, 2008.
14. C. Munoz-Camacho *et al.*, Phys. Rev. Lett.**97**, 262002, 2006.
15. S. Chen *et al.*, Phys. Rev. Lett.**97**, 072002, 2006.
16. A. Airapetian, et al., Phys. Rev. Lett. **87**, 182001, 2001.
17. R. De Masi et al., Phys. Rev. C**77**, 042201, 2008.
18. X. Ji, J.-P. Ma, F. Yuan, Nucl. Phys. B**652**, 383, 2003.
19. R. De Masi et al., Phys. Rev. C**77**, 042201, 2008.
20. JLab experiment E12-07-107, H. Avakian *et al.*.
21. JLab Experiment E03-12, H. Fenker, C. Keppel, S. Kuhn, W. Melnitchouk, *et al.*
22. JLAB Experiment E12-06-113, S. Bueltman *et al.*
23. X. Zheng *et al.*, Phys. Rev. C70, 065207, 2004.
24. V. Dharmawardane, *et al.*, Phys. Lett. B**641**, 11, 2006.
25. P. Bosted *et al.*, Phys. Rev. C**75**, 035203, 2007.
26. JLab experiment E12-06-109, S. Kuhn *et al.*
27. E. Leader, S. Sidorov, D. Stamenov, Phys. Rev. D**75**, 074027, 2007.
28. R. Fatemi *et al.*, Phys. Rev. Lett.**91**, 222002, 2003.
29. J. Yun *et al.*, Phys. Rev. C**67**, 055204, 2003.
30. M. Amarian et al., Phys. Rev. Lett. **92**, 022301, 2004.
31. A. Airapetian et al., Eur. Phys. J.C**26**, 527, 2003.
32. K. Abe *et al.*, Phys. Rev. D**58**, 112003, 1998.
33. P.L. Anthony *et al.*, Phys. Lett. B**493**, 19, 2000.
34. J.D. Bjorken, Phys. Rev. **148**, 1467, 1966.
35. V.D. Burkert, B.L. Ioffe, Phys. Lett. B**296**, 223, 1992.
36. V.D. Burkert, B.L. Ioffe, J. Exp. Theor. Phys.**78** , 619, 1994.
37. E. Thomas, N. Bianchi, Nucl. Phys. Proc.Suppl.**82**, 26, 2000.
38. M. Osipenko *et al.*, Phys. Rev. D**71**, 054007, 2005.
39. J.P. Chen, A. Deur, Z.-E. Meziani, Mod. Phys. Lett. A**20**, 2745, 2005.
40. A. Deur, *et al.*, Phys. Rev. Lett.**93**, 212001, 2004.
41. R. Hofstadter and R.W. Allister, Phys. Rev. **98**, 183, 1955.
42. V. Frolov *et al.*, Phys. Rev. Lett.**82**, 45,1999.
43. K. Joo, *et al.*, Phys.Rev. Lett. **88**, 122001, 2002.
44. M. Ungaro *et al.*, Phys. Rev. Lett.**97**, 112003, 2006.
45. C. Armstrong *et al.*, Phys. Rev. D**60**, 052004, 1999.
46. R. Thompson *et al.*, Phys. Rev. Lett.**86**, 1702, 2001.
47. H. Denizli *et al.*, Phys. Rev. C**76**, 015204, 2007.
48. K. Park *et al.*, Phys. Rev. C**77**, 015208, 2008.
49. I. Aznauryan et al., arXiv:0804.0447 [nucl-ex].
50. M. Ripani *et al.*, Phys. Rev. Lett.**91**, 022002, 2003.
51. V. Mokeev, invited talk presented at this conference.
52. T. Navasardyan et al., Phys. Rev. Lett. **98**, 022001, 2007.
53. K. Hafidi et al., in preparation.
54. The complete document may be obtained from the author.